

Spinodal and dynamical instabilities at the phase transition from the quark-gluon plasma to hadrons

P. Bożek*, Y.B. He and J. Hüfner

Institute for Theoretical Physics, University of Heidelberg, Philosophenweg 19, D-69120

Heidelberg, Germany

(November 20, 2018)

The stability of an expanding parton plasma is analyzed within quasi-particle models. The effective mass of the parton is calculated self-consistently from a gap equation which is either obtained from the Nambu Jona-Lasinio Lagrangian or from a fit to observables calculated on the lattice. The latter shows an effective confinement. At thermal equilibrium the stability is studied within thermodynamics (mechanical stability) and via a linear response analysis of the Vlasov equation. The instabilities related to a first-order phase transition are found. For a plasma expanding in three and one dimensions far from equilibrium a new type of instability, called dynamical, appears. The relation to cluster formation is shown in a molecular dynamics calculation.

PACS numbers: 25.75.-q, 12.38.Mh, 12.39.Ba

*On leave from: Institute of Nuclear Physics, Cracow, Poland

I. INTRODUCTION

The experimental search for the quark-gluon plasma in ultra-relativistic nuclear collisions requires the development of reliable and predictive models of the formation of the plasma and of its hadronization in order to be able to extract observables which signal the existence of a parton plasma in the high energy density region of the colliding nuclei. While lattice calculations have yielded important information on the equilibrium properties of a parton plasma (at least for baryon chemical potential $\mu = 0$), they are unable yet to describe the space-time development of the plasma formation and its subsequent decay into hadrons. The formation phase of the plasma is calculated usually in cascade models [1], which predict high values for the energy densities in the center of the collision. These values should be sufficient, according to lattice QCD calculations, for a plasma of deconfined quarks and gluons to be formed. A satisfactory microscopic calculation of the hadronization process in space-time is not yet available, in particular because of the complexity of the confinement problem. In this situation model studies are appropriate to elucidate the physics of the process. The present work is one of them.

In our work the partonic phase will be described within a quasi-particle model with an effective mass. The simplicity of the model allows to describe at the same time the equilibrium properties and the expansion dynamics. No hadronization is yet included. The medium dependent mass m (in the case of thermal equilibrium $m(T, \mu)$, and $m(x, t)$ for an expanding parton gas) is calculated self-consistently from a gap equation which relates the mass m to the local parton distribution function in phase space. The self-consistent mass itself determines the momentum distribution in the case of thermodynamical equilibrium or the evolution equation (the Vlasov equation) of the phase-space distribution in the nonequilibrium situation. We study two quasi-particle models, which are in a sense complementary:

1. The gap equation is the one of the Nambu Jona-Lasinio (NJL) model [2,3] with non-zero current quark mass. For $\mu = 0$ it shows a cross-over transition around a “critical” temperature T_c and a first one at low temperatures and finite baryon density.

2. We introduce a phenomenological parton model (PPM): Its gap equation is adjusted such that the quasi-particle model reproduces the lattice data for the energy density $\epsilon(T)$ and the chiral condensate $\langle\bar{\Psi}\Psi\rangle(T)$ around T_c (for $\mu = 0$) [4]. It is described in Ref. [5] and generalized to $\mu \neq 0$. It shows effective confinement in that the system cannot expand indefinitely, because the effective parton masses would grow to infinity.

For these two quasi-particle models we study the stability of the system in three physical situations.

- Within equilibrium thermodynamics the region in the plane of temperature T and baryon density ρ_B is calculated where $\partial P/\partial\rho_B < 0$, *i.e.*, the system is mechanically unstable. At the same time the region of the mixed phase in the T - ρ_B plane is calculated which indicates the presence of a first order phase transition.
- Using the method of linear response, the stability of the space-time dependent Vlasov equation around thermal equilibrium is investigated and the exponential growth rates are determined for the region of instability.
- The stability analysis of the Vlasov equation is also applied to situations far from equilibrium as they occur in three-dimensional (Hubble) and one-dimensional (Bjorken) expansions of a system of partons.
- In order to show that the instabilities are related to hadronization, we have studied the expansion and clusterization of an initially compact system of partons via molecular dynamics.

II. THE MODEL

The basic assumption of our work is the quasi-particle approximation for a gas of “partons” (quarks and gluons) with an effective medium dependent mass [4,5]. The thermodynamic potential of the quasi-particle system composed of fermions, antifermions and gluons with degeneracies g_f , $g_{\bar{f}} = g_f$ and g_g , respectively, is

$$P = \int \frac{d^3p}{(2\pi)^3} \frac{p^2}{3E} \left[g_f f_f(p) + g_f f_{\bar{f}}(p) + g_g f_g(p) \right] - V(m) , \quad (1)$$

where f_i is a Fermi or Bose distribution function and $V(m)$ is the mass dependent bag pressure. In our calculation we use the *same* effective mass for quarks and gluons. The parton mass depends on the medium through the gap equation :

$$\frac{dV}{dm} = - \int \frac{d^3p}{(2\pi)^3} \frac{m}{E} \left[g_f f_f(p) + g_f f_{\bar{f}}(p) + g_g f_g(p) \right] , \quad (2)$$

which follows from the thermodynamical relation

$$\frac{\partial P}{\partial m} = 0 . \quad (3)$$

Eq. (1) is not the most general expression for the pressure. For instance the bag pressure could also depend on the baryon density. Since lattice data are only available for zero baryon density, we cannot explore this possibility. For the NJL model, which has no gluons, the explicit form for dV/dm can be derived from the NJL Lagrangian within the mean field approximation. One has

$$\frac{dV}{dm} \equiv \frac{(m - m_0)}{2G} - g_f \int_{|p| < \Lambda} \frac{d^3p}{(2\pi)^3} \frac{m}{E} , \quad (4)$$

where G is the four fermion coupling constant, Λ a three-momentum cutoff, and m_0 the current quark mass. At zero baryon density the NJL model predicts a second order phase transition (for $m_0 = 0$) or a crossover behavior (for $m_0 > 0$) (see Fig. 1). At finite baryon density and low temperature the systems shows a first order phase transition for moderate values of the current quark mass (Fig. 2). We use the parameters $m_0 = 2$ MeV, $\Lambda = 653$ MeV and $G\Lambda^2 = 2.1$.

For the second model, called the phenomenological parton model (PPM) [5], the temperature dependence of the parton mass $m(T)$ is obtained by fitting the energy density

$$\epsilon = \int \frac{d^3p}{(2\pi)^3} E \left[g_f f_f(p) + g_f f_{\bar{f}}(p) + g_g f_g(p) \right] + V(m) \quad (5)$$

to lattice QCD data around T_c . The parton mass in the high temperature region $T \gg T_c$ is required to go smoothly towards zero in order to reproduce qualitatively the vanishing

chiral condensate at high temperature. For the present study we use the same procedure to obtain $m(T)$ as explained in Ref. [5], except that here we use Fermi and Bose distributions for the fermions and gluons, respectively, and take $g_f = 12$ corresponding to the two-flavor QCD. The energy scale is set by the critical temperature $T_c = 140$ MeV for the two-flavor QCD. Fig. 3 shows $m(T)$. Once it is known, one can use Eq. (2) to obtain dV/dm and V as a function of m . As explained in the beginning of this section, the quasi-particle model is completely defined once the bag pressure $V(m)$ is given. Fig. 4 compares the bag pressure $V(m)$ of the PPM model with the one of the NJL model. Note that we use $g_f = g_{\bar{f}} = 12$ in both models for the fermions, but for the gluons $g_g = 0$ in the NJL and $g_g = 16$ in the PPM model. The use of the Fermi and Bose distribution functions and the assumption that V depends only on m allow one to explore the parton mass and the thermodynamical properties of the system in the whole plane of temperature and baryon density, even where there are no lattice data. Fig. 5 shows the parton mass as a function of the chemical potential μ at $T = 100$ MeV for the phenomenological parton model. A first order phase transition is present at finite baryon density although at zero baryon density we have, following the lattice QCD, only a crossover behavior around T_c . This behavior, crossover transition at $\mu = 0$ and first order one at finite μ , is also found for the NJL model.

The quasi-particle models, whose thermodynamical properties are described above, can also be used to describe the space-time evolution of parton system. The underlying equation is the Vlasov one

$$\partial_t f_i(t, x, p) + \frac{\vec{p}}{E(t, x, p)} \cdot \nabla_x f_i(t, x, p) - \frac{m(t, x)}{E(t, x, p)} \nabla_x m(t, x) \cdot \nabla_p f_i(t, x, p) = 0, \quad (6)$$

where the quark, anti-quark or gluon distribution functions f_i at time t , at space point x and at three momentum p describe on-shell partons with energy $E = \sqrt{m^2 + \vec{p}^2}$. In a quasi-particle model there are no interactions between the quasi-particles, and therefore there are no collision terms on the r.h.s. of Eq. (6). The space-time dependent mass $m(t, x)$ is calculated self-consistently from the gap equation as a function of the non-equilibrium parton distribution functions $f_i(t, x, p)$:

$$\frac{dV}{dm} = - \sum_i g_i \int \frac{d^3p}{(2\pi)^3} \frac{m(t, x)}{E(p, t, x)} f_i(t, x, p) . \quad (7)$$

Eqs. (6) and (7) have to be solved simultaneously for an evolving parton gas. This has been done already for the phenomenological parton model with the result that during the expansion the partons acquire high masses and the expansion stops [5]. We call this behavior “effective confinement”.

III. MECHANICAL STABILITY AND FIRST ORDER PHASE TRANSITION

For a system at thermodynamic equilibrium the mechanical instability is defined by the condition

$$\left(\frac{\partial P}{\partial \rho_B} \right)_T < 0 . \quad (8)$$

With the gap equation (3) the condition (8) is equivalent to

$$\left(\frac{\partial \mu}{\partial \rho_B} \right)_T < 0 . \quad (9)$$

The negative derivative of the pressure or the chemical potential with respect to the density signals an instability of the homogeneous state of the system. Generally such an instability is related to a first order phase transition [6].

We discuss the numerical results for the two models, and begin with the NJL model. The pressure as a function of the baryon density is shown in Fig. 6 for several values of the temperature. For $T = 0$ for example the pressure is not a monotonic function of the density and a first order phase transition occurs. For the interval B–C in Fig. 6 the system is unstable since one has $\partial P / \partial \rho_B < 0$. The thermodynamical system is in a metastable state in the regions (intervals A–B and C–D in Fig. 6) around the unstable region. Performing a Maxwell construction amounts to choosing the correct solution of the gap equation for certain values of μ where the gap equation has 2 or 3 solutions for the mass (short dashed line in Fig. 6). The so constructed mass as a function of the chemical potential has a discontinuity at the critical chemical potential μ_c (see Fig. 2). The energy density and the

baryon density are also discontinuous at μ_c . The discontinuity in ρ_B means that the whole region AD of the baryon densities is excluded from the phase diagram. This region is called mixed phase and is shown in Fig. 7 in the plane of temperature and baryon density. The region of mechanical instability defined by Eq. (8) is a part of the mixed phase. Inside the region of mechanical instability the system is unstable with respect to non-homogeneous perturbations. In the whole region of mixed phase it is preferable for the system to separate into zones belonging to the low or high density thermodynamically stable phases.

For the phenomenological parton model, Fig. 8 shows the pressure as a function of the baryon density for several temperatures. The behavior is qualitatively similar to the NJL model: For $T < 120$ MeV the pressure is not a monotonic function of the density, and a Maxwell construction is required. However, quantitatively the situation for the PPM model is rather different and we have chosen the insert to show the situation for small ρ_B .

The regions of mechanical instability and metastability in the T - ρ_B plane are shown in Fig. 9 for the phenomenological parton model. A region with temperatures below 120 MeV and finite baryon density is unstable. As expected, for large temperature and/or baryon density the system is stable against mechanical perturbation, which is natural since then the partons are almost massless. However, the region around the y -axis ($\rho_B = 0$ and $T \geq 0$) is also stable.

The phenomenological parton model becomes questionable at values of T and ρ_B where the parton masses become much larger than the hadron masses, since hadronization is not accounted for. This is the case for the interior of the region of the mixed phase. However, close to the boundary of this region the model should correctly describe the thermodynamic situation including the effect of confinement.

Let us imagine a heavy ion collision and suppose that the system evolves at or close to thermal equilibrium: A region of deconfined parton plasma is created at high temperature and high baryon density in the stable regions of the phase diagrams in Figs. 7 or 9. During its expansion, the system reaches the region in the T - ρ_B plane where the local homogeneous parton distribution is unstable. In the spinodally unstable region any perturbation of the

homogeneous distribution amplifies and the system breaks up into regions (“clusters”) with larger density. This is the onset of hadronization. However, our quasi-particle models are not realistic in these regions, their and the structure, sizes and masses of the clusters cannot be reliably calculated. Sect. VII presents an illustration of the clusterization process.

IV. LINEAR INSTABILITY OF THE VLASOV EQUATION NEAR THERMAL EQUILIBRIUM

In the semi-classical limit the collisionless expansion of the plasma can be described by the Vlasov equations (6) together with the gap equation (7). In this section we address the linear stability problem of the Vlasov equation for the quasi-particle parton model around the equilibrium solution. We consider a small perturbation δf_i around the homogeneous solution f_i of the Vlasov equation :

$$f_i(t, x, p) = f_i(p) + \delta f_i(t, x, p) , \quad (10)$$

where the index i denotes the fermion, anti-fermion or gluon distribution. As it is standard practice [7,8], one linearizes the Vlasov equation and takes the Fourier transform in the t and x variables to obtain

$$(\vec{k} \cdot \vec{v} - \omega) \delta f_i(k, \omega, p) - \frac{m}{E} \delta m(k, \omega) \vec{k} \cdot \nabla_p f_i(p) = 0 , \quad (11)$$

where $\vec{v} = \vec{p}/E$, and $\delta m(k, \omega)$ is the change of the mass induced by the perturbation of the distribution functions δf_i , and has to satisfy the linearized gap equation

$$\delta \frac{dV}{dm}(k, \omega) = -\delta \left[\sum_i g_i \int \frac{d^3 p}{(2\pi)^3} \frac{m}{E} f_i(k, \omega, p) \right] . \quad (12)$$

This leads to

$$\frac{d^2 V}{dm^2} \delta m(k, \omega) = - \sum_i g_i \left[\int \frac{d^3 p}{(2\pi)^3} \frac{p^2}{E^3} f_i(p) \delta m(k, \omega) + \int \frac{d^3 p}{(2\pi)^3} \frac{m}{E} \delta f_i(k, \omega, p) \right] . \quad (13)$$

The fluctuation of the phase-space distributions $\delta f_i(\omega, k, p)$ can be expressed by the mass fluctuation $\delta m(k, \omega)$ using the linearized Vlasov equation (11)

$$\delta f_i(\omega, k, p) = \frac{m}{E} \frac{\partial f_i(E)}{\partial E} \frac{\vec{k} \cdot \vec{v}}{\vec{k} \cdot \vec{v} - \omega} \delta m(k, \omega) \quad (14)$$

and is inserted into the linearized gap equation:

$$\left[\frac{d^2 V}{dm^2} + \sum_i g_i \left[\int \frac{d^3 p}{(2\pi)^3} \frac{p^2}{E^3} f_i(p) + \int \frac{d^3 p}{(2\pi)^3} \frac{m^2}{E^2} \frac{\partial f_i(E)}{\partial E} \frac{\vec{k} \cdot \vec{v}}{\vec{k} \cdot \vec{v} - \omega} \right] \right] \delta m(k, \omega) = 0 . \quad (15)$$

The propagation of the disturbance δm is only possible, $\delta m \neq 0$, if ω and k are related, $\omega(k)$, such that the term in the square brackets is zero :

$$\frac{d^2 V}{dm^2} + \sum_i \frac{g_i}{2\pi^2} \left[\int_0^\infty \frac{p^4 dp}{E^3} f_i(p) + \int_0^\infty \frac{m^2 p^2 dp}{E^2} \frac{\partial f_i(E)}{\partial E} \chi\left(\frac{\omega}{kv}\right) \right] = 0 , \quad (16)$$

where

$$\chi(s) = 1 - \frac{s}{2} \ln \left(\frac{s+1}{s-1} \right) . \quad (17)$$

The dispersion relation $\omega(k)$ defined by Eq. (16) has two general properties. The solutions for the frequency ω come in pairs $\pm\omega$. The frequency is proportional to the wave-vector $\omega_k \sim k$, which is a general property as long as there is no scale in the dynamical equations. In our models the absence of scale is due to the fact that the relation between the density and the mass is local (zero-range interaction).

In the case of an imaginary solution of Eq. (16) for the frequency, $\omega_k = i\Gamma_k$, the initial disturbance grows exponentially in time

$$\delta f(x, t, p) \sim \exp(\Gamma_k t) , \quad (18)$$

i.e. an instability appears. As a consequence the system breaks up into smaller pieces. The fact that the instability rate is proportional to the wave-vector ($\Gamma_k \propto k$) means that the instability rates are unbounded, becoming arbitrary large for large k or small sizes. On the other hand we expect that the true clusters into which a low density parton system breaks up are the hadrons. The preference of the nature for the two or three quark clusters cannot be described in our simple model without color and with only local mean field interaction. A finite range of interaction or a minimal size of the cluster would regularize this unphysical

behavior. In that case there exists a maximal growth rate of instabilities for a specific wave-vector k [7]. We note that the presence of higher gradients in the dynamical equations would change the dispersion relation and limit the growth of excitations with large k [9]. In our case, the wave-vector for the physically most interesting instability, namely hadron formation, should be of the order of 1.0 fm^{-1} .

In the case of the stability analysis around thermal equilibrium, the instability observed in the Vlasov equation coincides with those of the mechanical instability and is thus related to the occurrence of a first order phase transition. Fig. 10 shows the contours of the growth rate Γ/k in the T - ρ_B plane for the phenomenological parton model. The region of $\Gamma/k > 0$ corresponds to the mechanical instability region studied in the previous section. The analysis based on the Vlasov equation thus reproduces the results of the thermodynamic analysis but goes further in that it also gives values of the growth rates in the unstable region. In the instability region close to the phase boundary, where we trust the model, calculated growth rates are of the order $\Gamma/k = 0.1$. For $k = 1.0 \text{ fm}^{-1}$ the instability growth time $1/\Gamma$ is of order $10 \text{ fm}/c$ and rather small on the time scale of nuclear reactions.

V. A GENERAL RESULT FOR THE CASE OF ZERO BARYON DENSITY

In this subsection we analyze the situation of finite T and $\rho_B = 0$. We prove that for any gap equation which yields $dm/dT < 0$, the Vlasov equation is stable against perturbations of the homogeneous equilibrium distribution. For $T > 0$ and $\rho_B = 0$ the dependence $m(T)$ of the mass on the temperature is obtained from the equilibrium gap equation

$$\frac{dV}{dm} = - \sum_i g_i \int \frac{d^3p}{(2\pi)^3} \frac{m}{E} F_i(E/T) , \quad (19)$$

where $F_i(E/T)$ is the equilibrium distributions for $\mu = 0$ written as a function of the variable E/T and

$$\frac{d^2V}{dm^2} = - \sum_i \frac{g_i}{2\pi^2} \left[\int_0^\infty \frac{p^4 dp}{E^3} F_i(E/T) + \int_0^\infty \frac{m}{TE} \left(\frac{m}{E} - \frac{dT}{T dm} \right) F'_i(E/T) \right] . \quad (20)$$

Inserting Eq. (20) into the relation (16) a dispersion relation for ω and k is obtained which depends on the derivative dm/dT :

$$\sum_i g_i \int p^2 dp F'_i(E/T) \left(\frac{m^2}{E^2} \left(1 - \chi\left(\frac{\omega}{kv}\right) \right) - \frac{m}{T} \frac{dT}{dm} \right) = 0 . \quad (21)$$

For any thermal distribution $F(E/T)$ its derivative $F'(E/T)$ is always nonzero and negative. The solutions for the collective frequency ω depend on the sign of dm/dT . Using the properties of the function $\chi(\omega/kv)$ for real and imaginary ω [8] one obtains

- In the case of $dm/dT > 0$, an imaginary solution of the dispersion cannot be excluded. However, no solution has been found for a version of the phenomenological parton model studied in Ref. [5], where the thermal mass increases at high temperatures. The absence of a solution can be traced to the fact that the thermal mass increases at high temperature only like

$$\frac{dm}{dT} < \frac{m}{T}. \quad (22)$$

- In the case of $dm/dT < 0$, there is no real or imaginary solution of the dispersion relation, and therefore the system is stable. This case applies to the two versions of the quasi-particle models studied in this paper, since $dm/dT < 0$ (Figs. 1 and 3). Any initial perturbation of the homogeneous distribution will be Landau damped and any oscillations or instabilities do not propagate or grow.

Note that the discussion is quite general. It applies to any effective quasiparticle theory of the type described in Sect. II, independently on the statistics of the particles and on the specific dependence of the mass on the temperature. In particular we confirm the results of Ref. [10] for the Nambu-Jona-Lasinio model at finite temperature and $\rho_B = 0$, where no instabilities have been found.

VI. LINEAR INSTABILITIES IN AN EXPANDING SYSTEM

In the previous sections the instabilities of the Vlasov equation are studied at thermal equilibrium within the NJL and the phenomenological parton models. While this analysis is

important in order to have a bridge to the condition of mechanical instability in equilibrium thermodynamics, it may not apply to the case of an expanding plasma, since situations far from equilibrium may occur, if thermalization is too slow. In the following we neglect thermalization altogether. We study the instabilities of a collisionless expanding plasma described by the Vlasov equation. The expansion of a thermal system quickly develops into a non-thermal distribution for which the instabilities may be of different nature. They appear also for $\rho_B = 0$. We study two examples of solutions for the Vlasov equation, the Hubble and Bjorken scenarios.

A. Three-dimensional expansion

The solution for an expansion in three dimensions, which is studied in this subsection, is called the Hubble solution, since it describes a homogeneous expansion where the local expansion velocity u_μ is proportional to the space-time vector x_μ . For the three-dimensional expansion of the plasma any function

$$f(p, x, t) = f_0(s) \quad (23)$$

of the variable

$$s = \frac{\tau}{\tau_0} \sqrt{(p^\mu u_\mu)^2 - m(\tau)^2} \quad (24)$$

solves the Vlasov equation, and the mass depends only on the proper time $\tau = \sqrt{t^2 - \vec{x}^2}$ and $u_\mu = x_\mu/\tau$ is the local expansion velocity [11]. If the system is in thermal equilibrium at the initial proper time τ_0 with mass $m(\tau_0)$ then the solution can be written in the form

$$f(p, x, t) = F(\sqrt{s^2 + m(\tau_0)^2}/T) , \quad (25)$$

where $F(x) = \exp(-x)$ is the thermal distribution function (In this section we restrict ourselves only to Boltzmann statistics, since we consider the case $\mu = 0$. We have checked that the stability condition and the instability growth rates are not much affected by the

statistics.). For the case $m(\tau_0) = 0$, f is only a function of s/T for all space-time points. In the local rest frame $\vec{x} = 0$, $\tau = t$ one has $s = |\vec{p}|\tau/\tau_0$ and

$$f(p, \tau) = F(|\vec{p}|\tau/T\tau_0) \quad (26)$$

for all times. This distribution is a thermal one with time-dependent temperature $T(\tau) = T\tau_0/\tau$, provided the mass remains zero. However the self-consistent mass $m(\tau)$ calculated from the gap equation

$$\frac{dV}{dm} = -g \int \frac{d^3p}{(2\pi)^3} \frac{m}{E} F(p\tau/T\tau_0) \quad (27)$$

increases rapidly with time τ (Fig. 11). In this case $F(p\tau/T\tau_0)$ is no more a thermal distribution. In order to analyze the stability of the solution (26) we linearize the Vlasov and the gap (27) equations. The procedure leads to a complicated expression, since both the zero order solution $F(s/T)$ and the linear perturbation δf depend on space and time. If we restrict ourselves to the vicinity of the point $\vec{x} = 0$, the linearized Vlasov equation simplifies, since the \vec{x} -dependence of the zero order solution is weak:

$$\partial_t \delta f(p, x, t) + \frac{\vec{p}}{E(\tau)} \cdot \nabla_x \delta f(p, x, t) - \frac{m(\tau)}{E(\tau)} \nabla_x \delta m(x, t) \cdot \nabla_p F(p\tau/T\tau_0) = 0, \quad (28)$$

where now $\tau = t$. If one wants to proceed as in Sect. IV and introduces the Fourier transforms of δf and δm with respect to \vec{x} and t , one has to neglect the time dependence of the zero order solution $F(p\tau/T\tau_0)$ and $m(\tau)$ in comparison to the expected stronger time variation of the perturbation $\delta f(p, x, t)$. This is equivalent to an adiabatic approximation considering τ as an external parameter which changes the properties of the medium. After Fourier transformation one obtains the familiar form of the linearized Vlasov equation

$$(\omega - \vec{k} \cdot \vec{v}) \delta f(p, k, \omega) + \frac{m}{p} \vec{k} \cdot \vec{v} \partial_p F(p\tau/T\tau_0) \delta m = 0. \quad (29)$$

Together with the gap equation (27) one gets the dispersion relation in the form:

$$\int_0^\infty \frac{p}{E} dp F'(p\tau/T\tau_0) \left(\chi\left(\frac{\omega}{kv}\right) - p^2 \frac{d \ln(\tau/\tau_0)}{m dm} \right) = 0, \quad (30)$$

which has an imaginary solution for the frequency if

$$\int_0^\infty \frac{p}{E} dp F'(p\tau/T\tau_0) \left(1 - p^2 \frac{d \ln(\tau/\tau_0)}{m dm} \right) > 0 . \quad (31)$$

The dispersion relation (30) determines the ratio ω/k . For $\Gamma_k > 0$ one has an exponentially growing instability. Fig. 12 shows the growth rate of the instability as a function of the expansion time τ/τ_0 . If we chose a typical value $k = 1.0 \text{ fm}^{-1}$, the growth rate refers to a spinodal instability of the size 1 fm. At $\tau/\tau_0 = 1.9$ the system becomes unstable and quickly reaches a regime of rather short instability time scales of order $1/\Gamma = 1.0 \text{ fm}/c$.

A necessary condition for the appearance of the linear instabilities in the expanding plasma is that the mass increases significantly around T_c . For example we have found that the linear instabilities do not appear for the NJL model or for the three-dimensional Hubble expansion in the phenomenological parton model where the parton mass in vacuum is taken smaller than $\sim 3T_c$. Note that an instability develops for the case $\rho_B = 0$, although there is no first order phase transition as discussed above.

B. One-dimensional expansion

For a one dimensional homogeneous expansion of the plasma (Bjorken scenario) the Vlasov equation is solved by any function of the scaling variable s and of the transverse momentum p_\perp [11]

$$f(p, x, t) = f_0(s, p_\perp) , \quad (32)$$

with

$$s = \frac{\tau}{\tau_0} \sqrt{(p^\mu u_\mu)^2 - p_\perp^2 - m(\tau)^2} \quad (33)$$

and $u_\mu = (t, 0, 0, z)/\tau$. In the local rest frame ($z = 0$) and for a thermal initial state with $m(\tau_0) = 0$ the one-dimensional solution takes the form

$$f(p, x, t) = F(\sqrt{(\tau p_\parallel/\tau_0)^2 + p_\perp^2}/T) = F(E_\tau/T) . \quad (34)$$

The mass $m(\tau)$ can be calculated from the gap equation and is shown in Fig. 11. In the one-dimensional case the mass increases more slowly than in the three-dimensional case since only the longitudinal momentum is dilated.

Linearizing around the one-dimensional homogeneous expansion, we consider two kinds of perturbation, longitudinal $\delta f(p, z, t)$ and transverse $\delta f(p, x_\perp, t)$ ones. Any general linear solution of the Vlasov equation can be factorized into the transverse and the longitudinal ones. The approximations in deriving the dispersion relation from the linearized Vlasov and gap equations are the same as in the three-dimensional case. One obtains

$$\int_0^\infty p_\perp dp_\perp \int_{-\infty}^\infty dp_\parallel \frac{F'(E_\tau/T)}{EE_\tau} \left[\frac{k_\parallel v_\parallel}{\omega - k_\parallel v_\parallel} + p_\parallel^2 \frac{d \ln \tau / \tau_0}{mdm} \right] = 0 , \quad (35)$$

where $v_\parallel = p_\parallel/E$ and k_\parallel is the longitudinal wave-vector of the perturbation. The above equation has a purely imaginary solution $\omega = \pm i\Gamma$ if

$$\int_0^\infty p_\perp dp_\perp \int_{-\infty}^\infty dp_\parallel \frac{F'(E_\tau/T)}{EE_\tau} \left[1 - p_\parallel^2 \frac{d \ln \tau / \tau_0}{mdm} \right] > 0 . \quad (36)$$

In the transverse direction the dispersion relation reads

$$\int_0^\infty p_\perp dp_\perp \int_0^{2\pi} d\phi \int_{-\infty}^\infty dp_\parallel \frac{F'(E_\tau/T)}{EE_\tau} \left[\frac{k_\perp v_\perp \cos \phi}{\omega - k_\perp v_\perp \cos \phi} + p_\parallel^2 \frac{d(\tau/\tau_0)^2}{dm^2} \right] = 0 , \quad (37)$$

where k_\perp is the transverse wave-vector of the perturbation. The transverse dispersion relation has a purely imaginary frequency solution if

$$\int_0^\infty p_\perp dp_\perp \int_{-\infty}^\infty dp_\parallel \frac{F'(E_\tau/T)}{EE_\tau} \left[1 - p_\parallel^2 \frac{d(\tau/\tau_0)^2}{dm^2} \right] > 0 . \quad (38)$$

Comparing the conditions for the longitudinal and transverse instabilities (Eqs. (36) and (38)) one finds that the system becomes unstable first in the longitudinal direction, since

$$\frac{d(\tau/\tau_0)^2}{dm^2} > \frac{d \ln \tau / \tau_0}{mdm} . \quad (39)$$

Furthermore the longitudinal instability growth rate is larger than the transverse one. Fig. 12 shows the time dependence of the longitudinal instability growth rate for the one-dimensional expansion. The growth rate Γ is much smaller than in the three-dimensional case and is

comparable to the growth rates in equilibrium at finite baryon density. For the wave-vector $k = 1.0 \text{ fm}/c$ one has a maximum value of $\Gamma \simeq 0.5 \text{ c}/\text{fm}$ at $\tau/\tau_0 = 8$. The transverse perturbation remains stable for the phenomenological parton model.

VII. CLUSTERIZATION IN A MOLECULAR DYNAMICS CALCULATION

When a perturbation of the zero order Vlasov equations is unstable, the linear approximation breaks down for larger times. The development of the instabilities beyond the linear approximation can only be studied numerically. In the case of the mean field evolution (Vlasov equation), the numerical noise due to the finite number of test particles is a big problem [12]. It is very difficult to disentangle the numerical noise from the true fluctuations of the system acting as a seed for the development of the unstable modes. We have not attempted to solve this problem. Instead we study a different but closely related model. It is the molecular dynamical model with medium dependent masses. The local mean-field approximation to this model reduces to the Vlasov equation studied in the previous section. The model deals with classical partons whose masses are related to the density in the vicinity. The time dependent positions $\vec{x}_i(t)$ and momenta $\vec{p}_i(t)$ of the N partons follow Hamilton's equations

$$\begin{aligned}\frac{d\vec{p}_i}{dt} &= -\frac{m_i}{E_i} \nabla_x m_i \\ \frac{d\vec{x}_i}{dt} &= \frac{\vec{p}_i}{E_i}.\end{aligned}\tag{40}$$

The parton mass is calculated from the gap equation with the scalar density in its vicinity. This requires the introduction of a range over which the density is calculated. We define the scalar density at position $\vec{x}_i(t)$ at time t by

$$\rho_s(\vec{x}_i(t)) = \frac{1}{(2\pi\sigma)^{3/2}} \sum_{j \neq i} \frac{m_j}{E_j} e^{-(\vec{x}_i - \vec{x}_j)^2 / 2\sigma^2},\tag{41}$$

where the sum runs over all the particles j (with positions $\vec{x}_j(t)$, masses $m_j(t)$ and energies $E_j(t)$) other than the parton i . It determines the mass of the parton i through the gap equation of the phenomenological parton model

$$\frac{dV(m_i)}{dm} = -\rho_s(\vec{x}_i(t)) . \quad (42)$$

The introduction of the finite range σ (which we take $\sigma = 0.5$ fm) has important consequences: (i) For a finite value of σ , the mass of particle i at \vec{x}_i and t cannot be determined by the masses of the particles j at the same time t , but only at earlier times (causality). As long as the masses vary slowly with time, the violation of causality may have no dramatic consequences. (ii) The size of the clusters into which the system breaks up will be strongly influenced by the value of σ , but we have not yet studied this dependence.

Using the gap equation for the phenomenological parton model, we have performed a simulation using 100 partons with initial temperature $T = 180$ MeV distributed in a fireball of radius $r_0 = 2$ fm. The system expands and its density drops. Fig. 13 presents the evolution of the system at different times by showing the positions (x, y) of the partons projected on the $z = 0$ plane. The partons tend to stay grouped in regions and structures of large local density. Eventually as the expansion proceeds the partons group themselves into compact clusters composed of at least two partons. There are no single partons. This is as close as one can do with the hadronization process in a model which does not know of color and not of quantum mechanics. The qualitative picture obtained from this calculation corresponds to the final stage of the dynamical break up of the system, which manifest itself first as a linear instability studied in the previous sections. The molecular dynamics evolution follows the system for times beyond the applicability of the linear response.

VIII. SUMMARY AND CONCLUSIONS

We have studied the instabilities of a plasma of partons. The plasma is treated in a quasi-particle model with an effective mass m , which depends on T and μ in the equilibrium situation and on \vec{x} , t for the expansion. The gap equation which relates the mass to the scalar density of the partons defines the underlying dynamics. We have studied two cases in parallel: (i) a gap equation derived from the NJL-Lagrangian in the mean field approximation and (ii) a phenomenological gap equation which is chosen so that certain

observables calculated from the lattice are reproduced by the quasi-particle model. While both models show a crossover transition for $\mu = 0$ and a first order phase transition for $\mu \neq 0$, only the phenomenological model has properties of confinement, in that the parton mass becomes very large for vanishing density. The study of these two, in some sense, complementary models, permits to get an idea on the model dependence of the results. The stability analysis has been performed on four levels:

- For thermal equilibrium, one calculates the regions in the $T - \rho_B$ plane, in which the system is stable, metastable and unstable. These regions are calculated starting from the pressure as a function of T and ρ_B . At thermal equilibrium instabilities are expected only at and due to the first order phase transitions. Since both models, the NJL and the phenomenological one show a first order phase transition for certain values of T and ρ_B , the phase diagrams look rather similar from a qualitative point of view, but the values of T and ρ_B at the phase boundaries are rather different.
- Another interesting result found from the analysis of the phase diagram of the phenomenological parton model is the presence of the first order phase transition at finite baryon densities. Although we have followed the lattice QCD data at zero baryon density which show only a crossover transition around T_c the generalization to finite baryon density using a gap equation depending only on the scalar density leads to a first order phase transition. This simple model shows that the occurrence of a first order phase transition in the highly excited matter with finite baryon density created in ultrarelativistic heavy ion collisions cannot be excluded from the lattice QCD data at zero baryon density.
- The growth rates for the instabilities found in the thermodynamic analysis can be calculated from the Vlasov equation in a linear response analysis around thermal equilibrium. The neglect of the collisions in the linear response analysis in this work is justified when the instability growth rate is larger than the equilibration rate. We prove that for any quasi-particle model for which $dm/dT < 0$, one has a stable system

for $\rho_B = 0$. In general the dispersion relation for frequency ω and wave vector k of the instability has no scale and gives $\omega \propto k$, since the gap equation corresponds to a zero range interaction. In the region of the mixed phase obtained from equilibrium thermodynamics, one finds solutions with $\text{Im}\omega > 0$, *i.e.*, perturbations which grow exponentially in time. For the typical scale corresponding to the wave vectors $k \simeq 1.0 \text{ fm}^{-1}$ and as long as one is not too far away from the phase boundary¹ the value of the growth rate $\text{Im}\omega \simeq 0.1 \text{ (fm/c)}^{-1}$ is surprisingly small (compared to the expansion time scale of the plasma).

- The stability behavior far from equilibrium has been studied by investigating the Hubble- and Bjorken-solutions, (*i.e.*, three- and one-dimensional expansion, respectively) of the Vlasov equation again by the method of linear response. The condition for the validity of this procedure is that the growth rate of the instability is faster than the expansion time (which itself must be larger than the relaxation time in order to be able to use the collisionless Vlasov equation). No instabilities are found for the NJL-model, while the phenomenological model quickly ($\tau \geq 2\tau_0$) develops instabilities with significant growth rates ($\text{Im}\omega \simeq 0.5$ to 1.0 (fm/c)^{-1} for $k = 1.0 \text{ fm}^{-1}$) even for $\rho_B = 0$. We call these instabilities dynamical ones, since they are obviously not related to the first order phase transition but rather to the confinement properties of the phenomenological quasi-particle model.
- The analysis of the instabilities based on linear response, be it at thermal equilibrium or for an expansion far from equilibrium, is limited to small times, if one finds exponential growth. The behavior over large times can only be studied numerically. We have attempted a first step in this direction, in that we have followed the expansion of a plasma described by the phenomenological quasi-particle model in a molecular

¹The models based solely on the parton degrees of freedom may have not much physical meaning far in the confined phase.

dynamical calculation. We find indeed that the expansion of the system eventually leads to clusters with at least two partons. This is as far as one can get in a classical model which does not know color degrees of freedom. More work in this direction is intended.

ACKNOWLEDGMENTS

The authors thank Hilmar Forkel and Gábor Papp for several helpful discussions. P.B. thanks the A.v. Humboldt foundation for financial support. Y.B.H. is supported by the grant 06 HD742 from the German Federal Ministry of Education and Research. J.H. is grateful to A. Gal and the Physics Department of the Hebrew University for their hospitality and support during a stay where some this work has been done.

-
- [1] K. Werner, Phys. Rep. **232**, 87 (1993); H. Sorge, Phys. Rev. C **52**, 3291 (1995); Y. Pang, T.J. Schlagel and S.H. Kahana, Nucl. Phys. **A544**, 435 (1992); K. Geiger, Phys. Rep. **258**, 237 (1995); X.-N. Wang and M. Gyulassy, Phys. Rev. D **44**, 3501 (1991).
 - [2] Y. Nambu and G. Jona-Lasinio, Phys. Rev. **122**, 345 (1961); **124**, 246 (1961).
 - [3] For recent reviews, see *e.g.*, U. Vogl and W. Weise, Prog. Part. Nucl. Phys. **27**, 195 (1991); S.P. Klevansky, Rev. Mod. Phys. **64**, 649 (1992); T. Hatsuda and T. Kunihiro, Phys. Rep. **247**, 221 (1994).
 - [4] M.I. Gorenstein and S.N. Yang, Phys. Rev. D **52**, 5206 (1995); A. Peshier, B. Kämpfer, O.P. Pavlenko and G. Soff, Phys. Rev. D **54**, 2399 (1996); P. Lévai and U. Heinz, hep-ph/9710463.
 - [5] P. Božek, Y.B. He and J. Hüfner, Phys. Rev. C **57**, 3263 (1998).
 - [6] L.D. Landau and E.M. Lifschitz, *Statistical Physics*, Pergamon (London, 1969).
 - [7] G. Bertsch and P. Siemens, Phys. Lett. B **126**, 9 (1983); J. Cugnon, Phys. Lett. B **135**, 374

- (1984); H. Heiselberg, C.J. Pethick and D.G. Ravenhall, Phys. Rev. Lett. **61**, 818 (1988); M. Colonna, P. Chomaz and J. Randrup, Nucl. Phys. A **567**, 637 (1994); L.P. Csernai, J. Németh and G. Papp, Heavy Ion Phys. 3 (1996) 17.
- [8] C.J Pethick and D.G. Ravenhall, Ann. Phys. **183**, 131 (1988).
- [9] S. Ayik, M. Colonna and P. Chomaz, Phys. Lett. B **353**, 417 (1996).
- [10] W. Florkowski, Phys. Rev. C, 3069 (1994).
- [11] L.P Csernai and I.N. Mishustin, Phys. Rev. Lett. **74**, 5005 (1995); I.N. Mishustin and O. Scavenius, Phys. Lett. B **396**, 33 (1997).
- [12] G.F Burgio, Ph. Chomaz and J. Randrup, Nucl. Phys. A **529**, 157 (1991); E. Suraud, S. Ayik, M. Belkacem and J. Stryjewski, Nucl. Phys. A **542**, (1992); G.F. Burgio, Ph. Chomaz and J. Randrup, Phys. Rev. Lett. **73**, 3512 (1994).

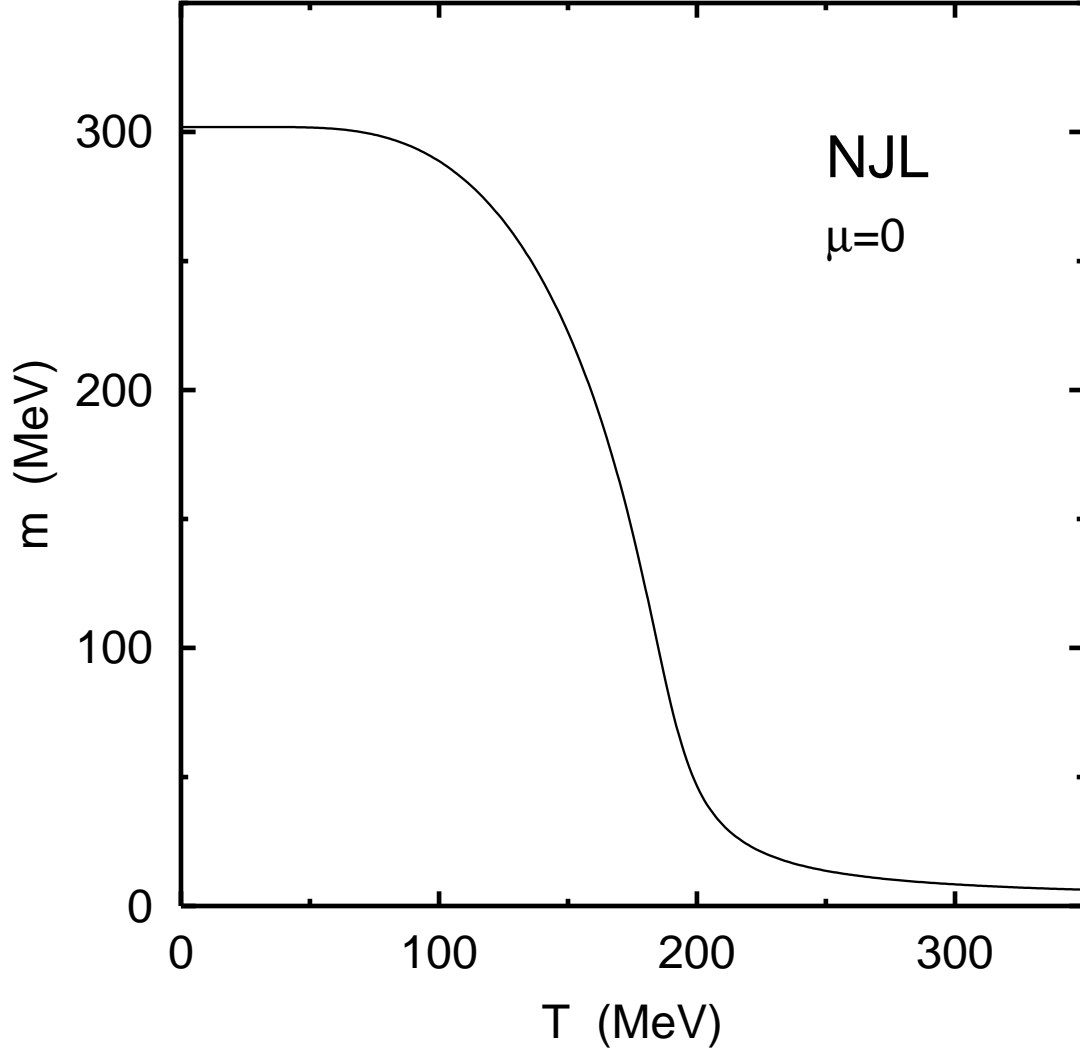


FIG. 1. The temperature dependence of the parton mass in the two-flavor NJL model for $\mu = 0$.

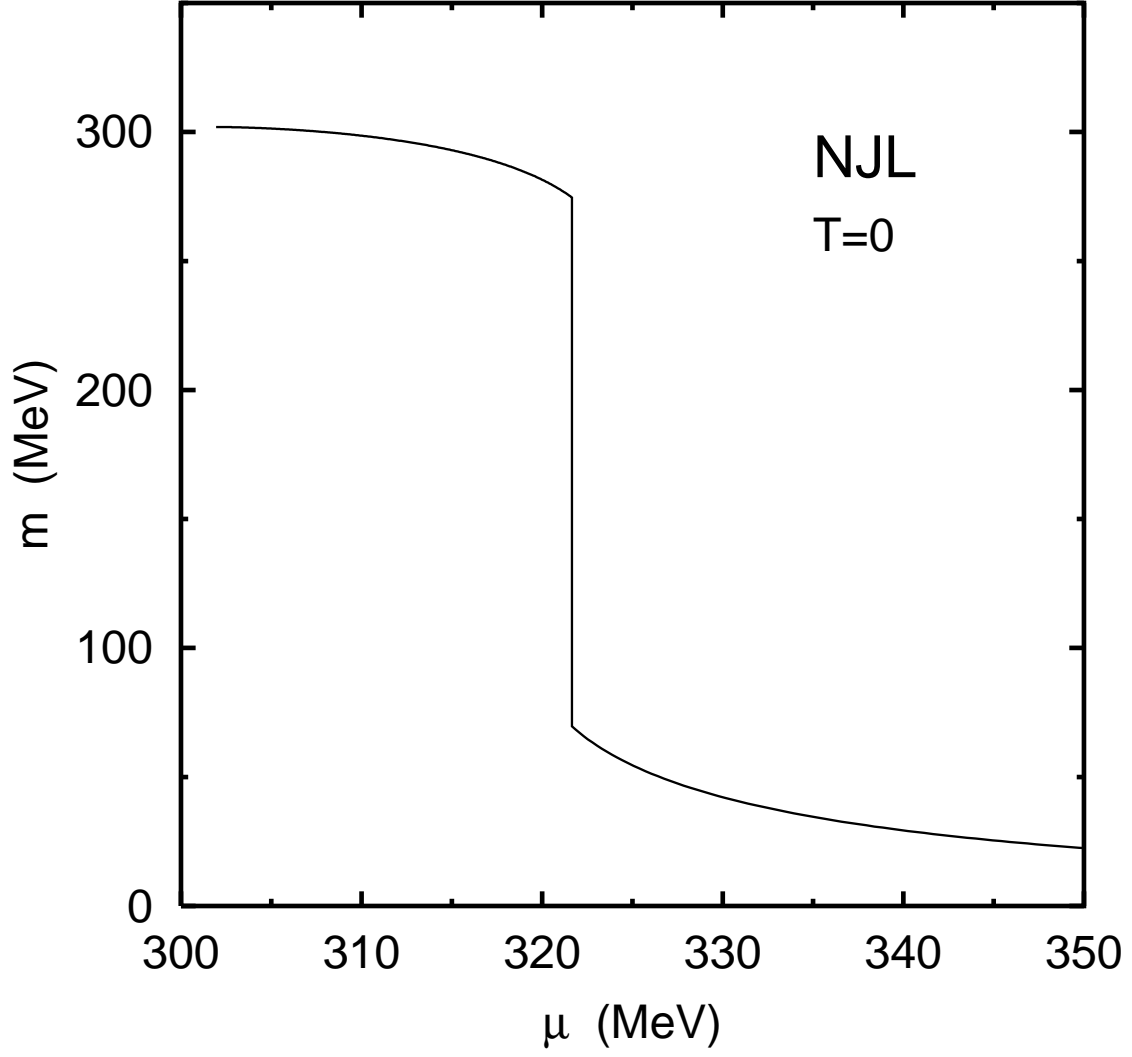


FIG. 2. The dependence of the parton mass on the chemical potential in the NJL model at $T = 0$. Note the expanded scale on the abscissa.

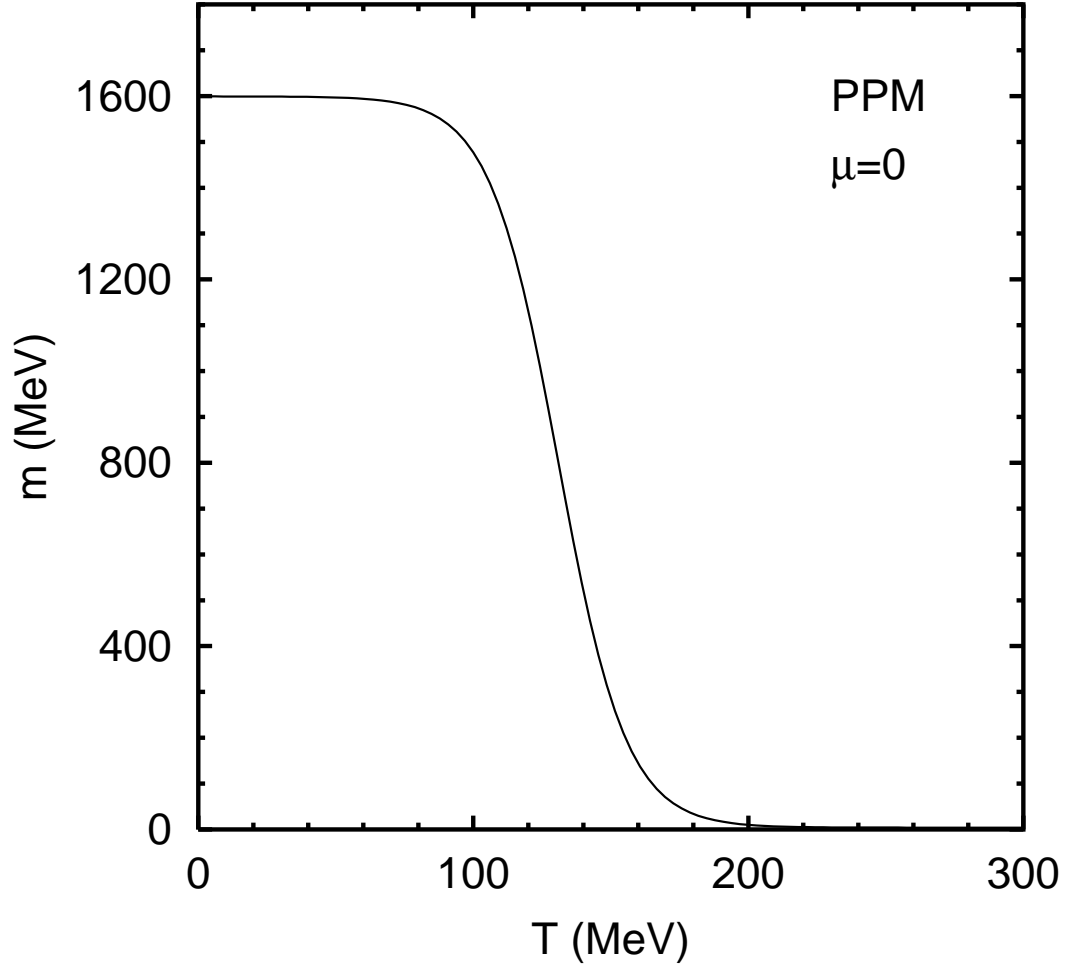


FIG. 3. The temperature dependence of the parton mass in the phenomenological parton model (PPM) at $\mu = 0$.

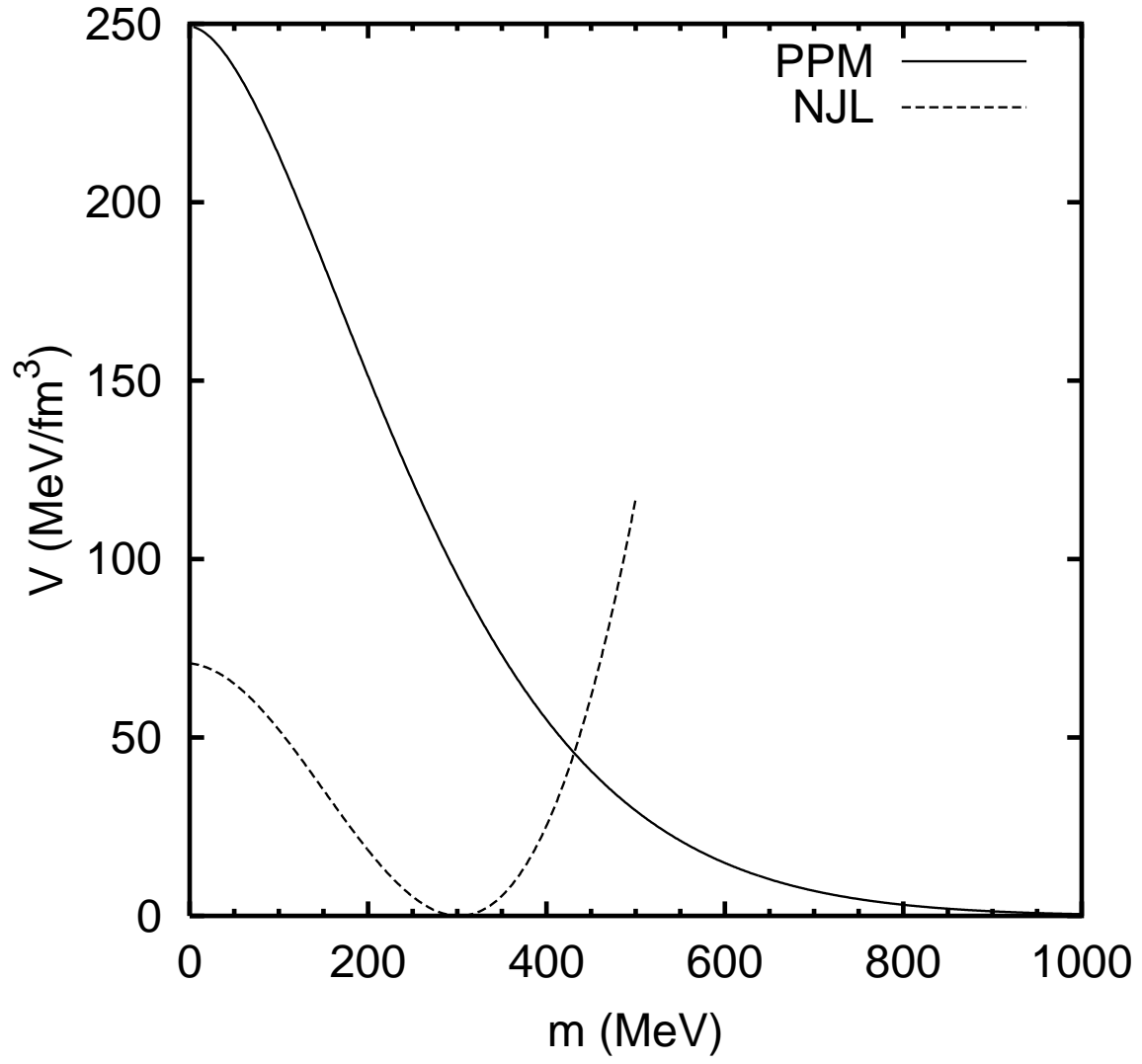


FIG. 4. The bag pressure density V as a function of the effective mass for the NJL model (dashed curve), and for the phenomenological parton model (solid curve).

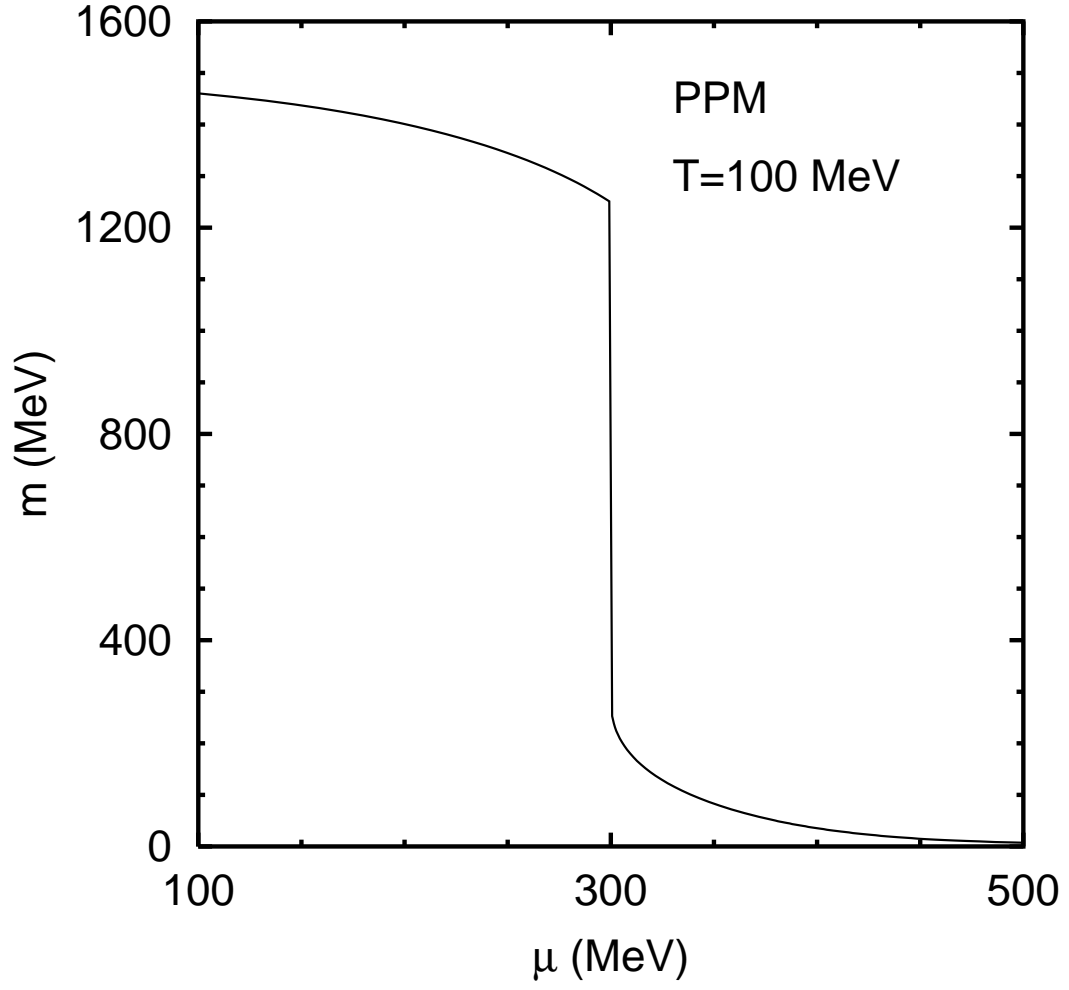


FIG. 5. The dependence of the parton mass on the chemical potential in the phenomenological parton model at $T = 100$ MeV.

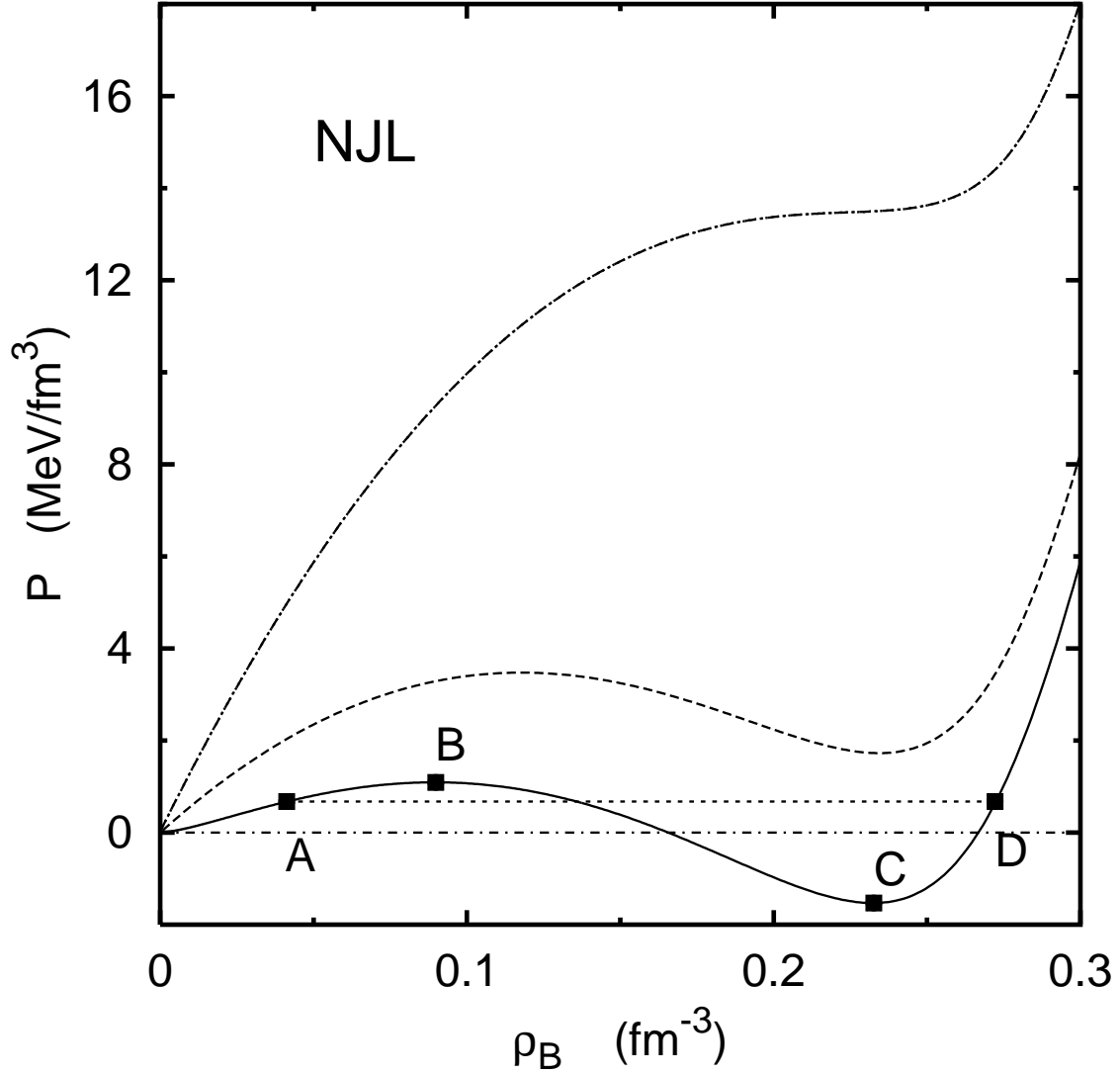


FIG. 6. The pressure density as a function of the baryon density in the NJL model for $T = 0$, 20 and 45 MeV, solid, dashed and dash-dotted lines, respectively. The parts A–B and C–D of the $T = 0$ curve correspond to the metastable states and the part B–C to the unstable state of the system. The straight line from A to D is the Maxwell construction for $T = 0$. A similar classification into unstable and metastable regions can be made for $T = 20$ MeV. For $T = 45$ MeV the system shows no first order transition.

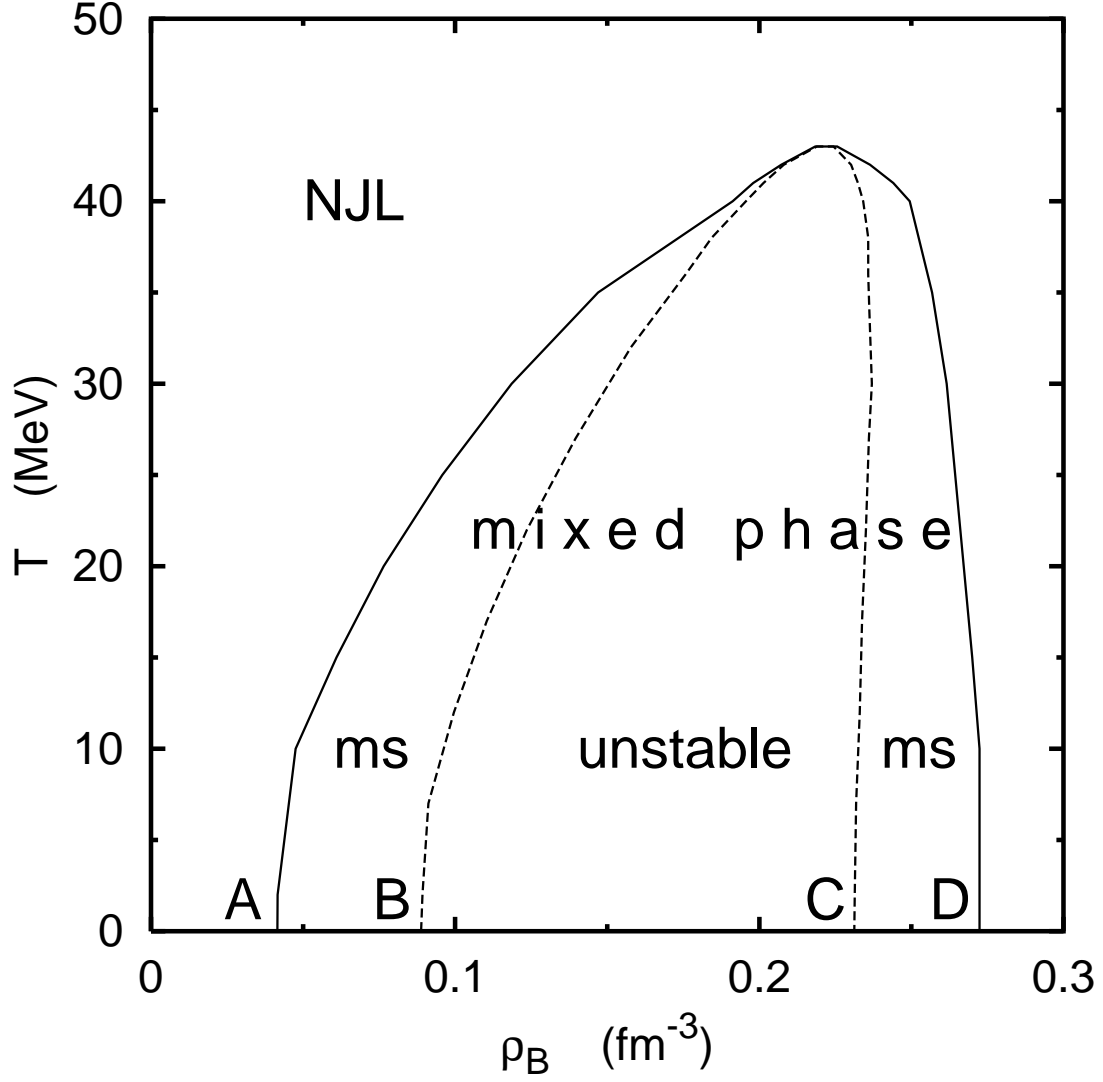


FIG. 7. The solid line in the $T - \rho_B$ plane separates the stable region and the mixed phase. The mixed phase is divided into regions of instability (“unstable”) and metastability (“ms”). The letters A to D at the bottom relate to $T = 0$ and correspond to the points in Fig. 6. The results are for the NJL model.

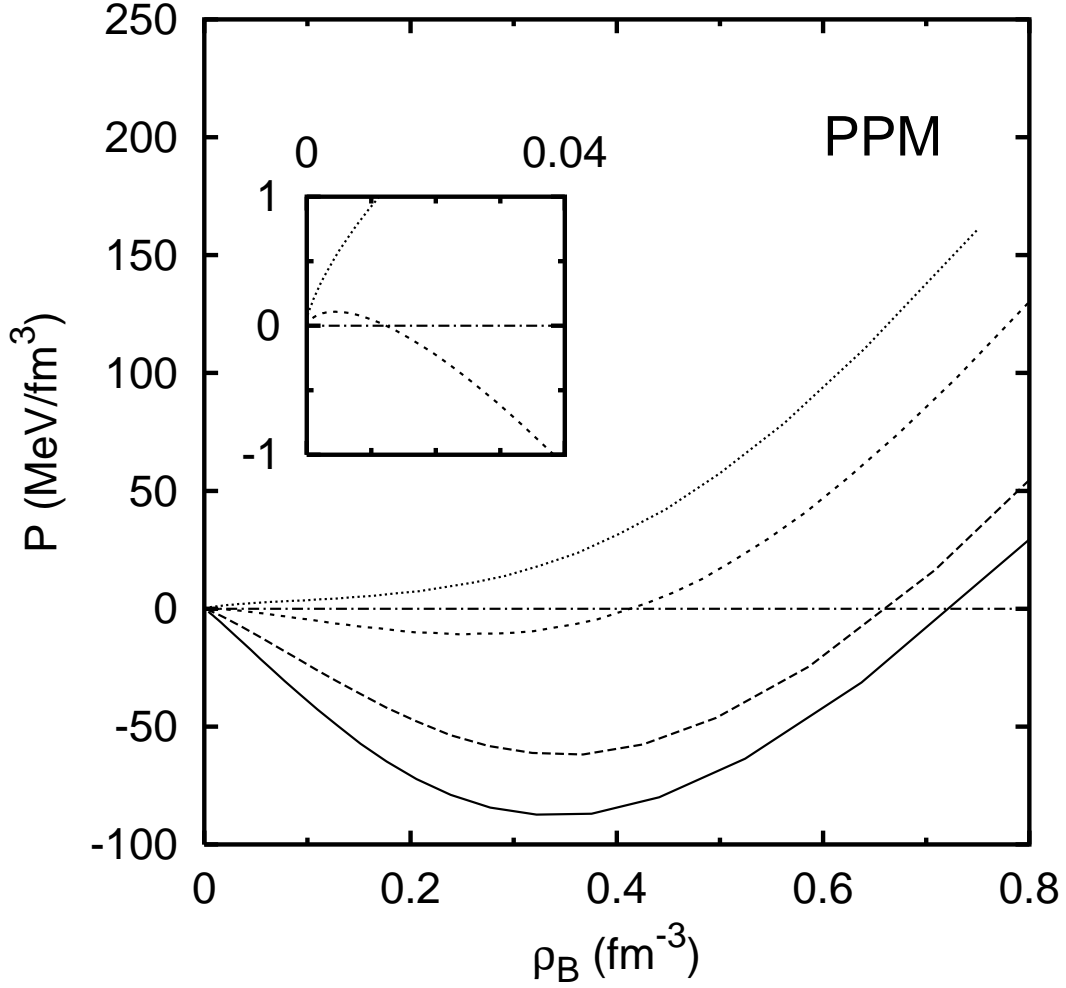


FIG. 8. The pressure density as a function of the baryon density in the phenomenological parton model at different temperatures. The four curves (from bottom to top) correspond to temperatures $T = 0, 50, 100, 120$ MeV, respectively, while the insert magnifies the details around the origin for temperatures $T = 100$ and 120 MeV.

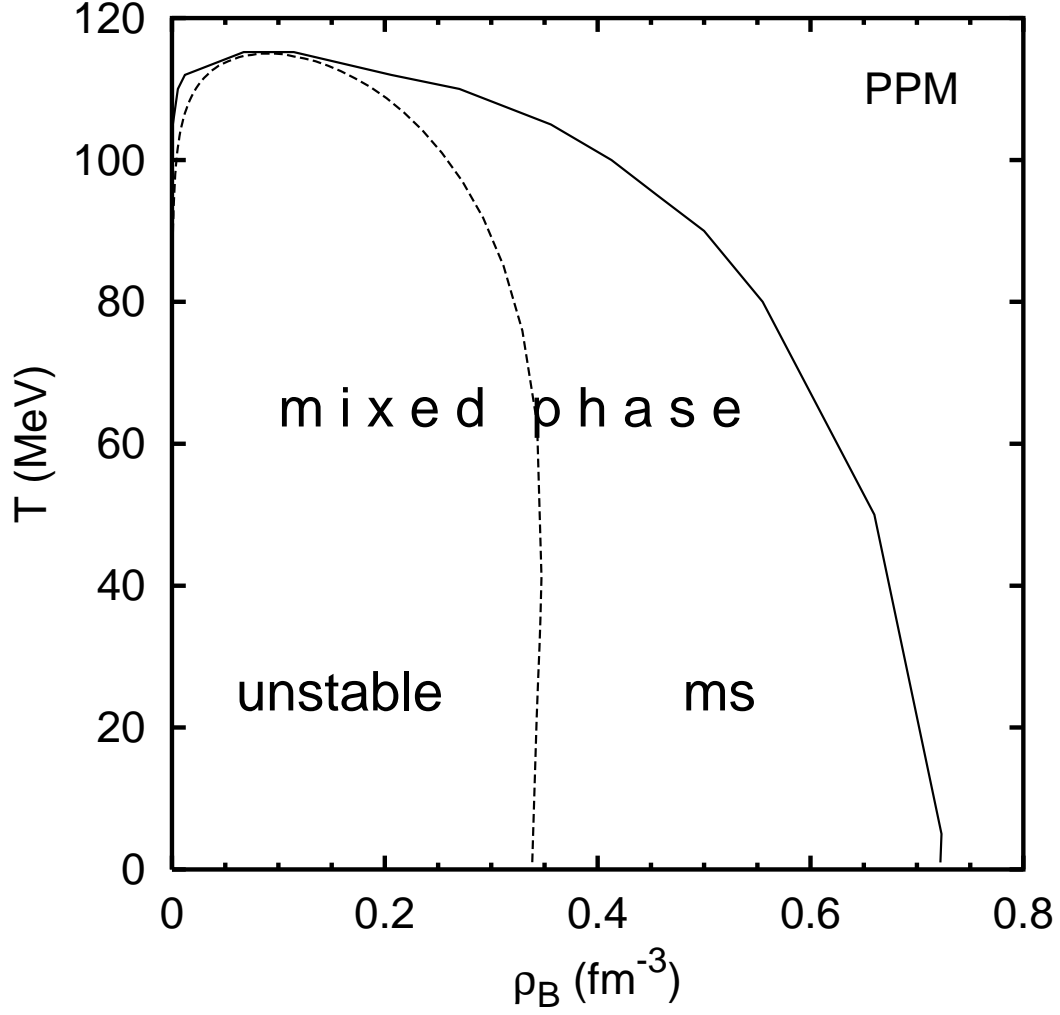


FIG. 9. The regions of the mixed, unstable and metastable phases in the $T - \rho_B$ plane in the phenomenological parton model. Note that the whole line $\rho_B = 0$ is part of the stable region.

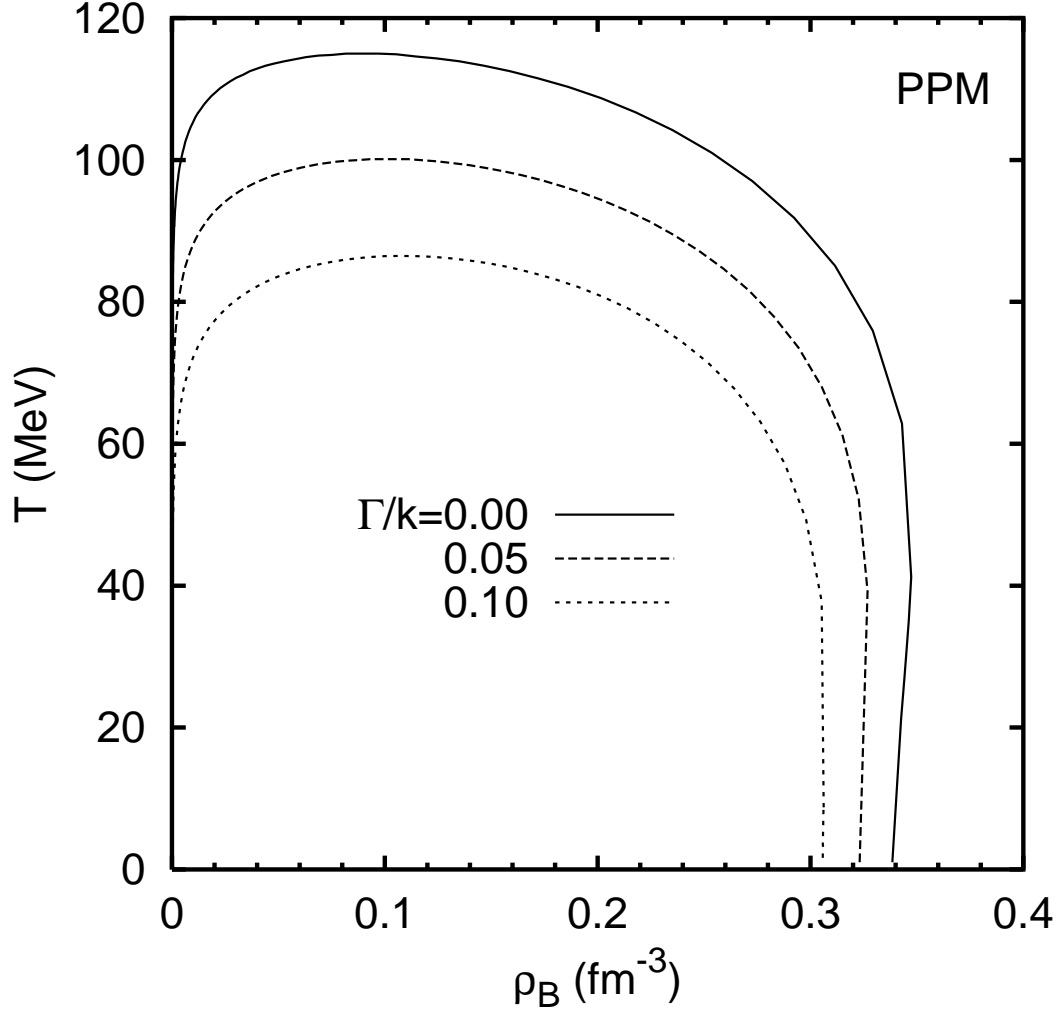


FIG. 10. The contour plots for the instability growth rate Γ divided by the wave vector k in the T - ρ_B plane for the phenomenological parton model. The solid line of this figure corresponds to the dashed one in the previous figure, which is the border of mechanical instability region.

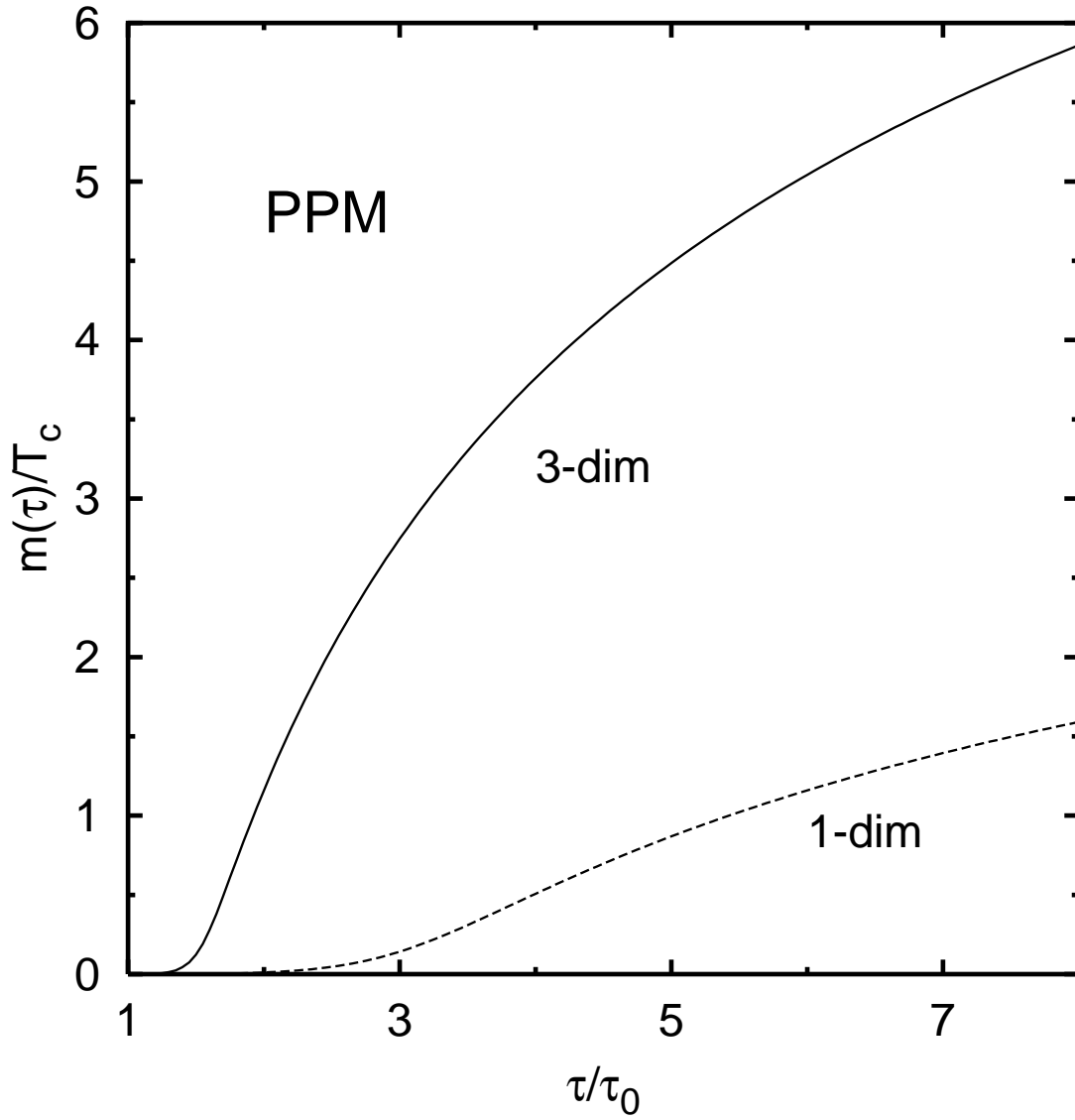


FIG. 11. The parton mass as a function of the proper time for the three-dimensional homogeneous expansion (solid line) and for the Bjorken expansion (dashed line). At $\tau/\tau_0 = 1$ one has a thermal distribution with $T = 2T_c$.

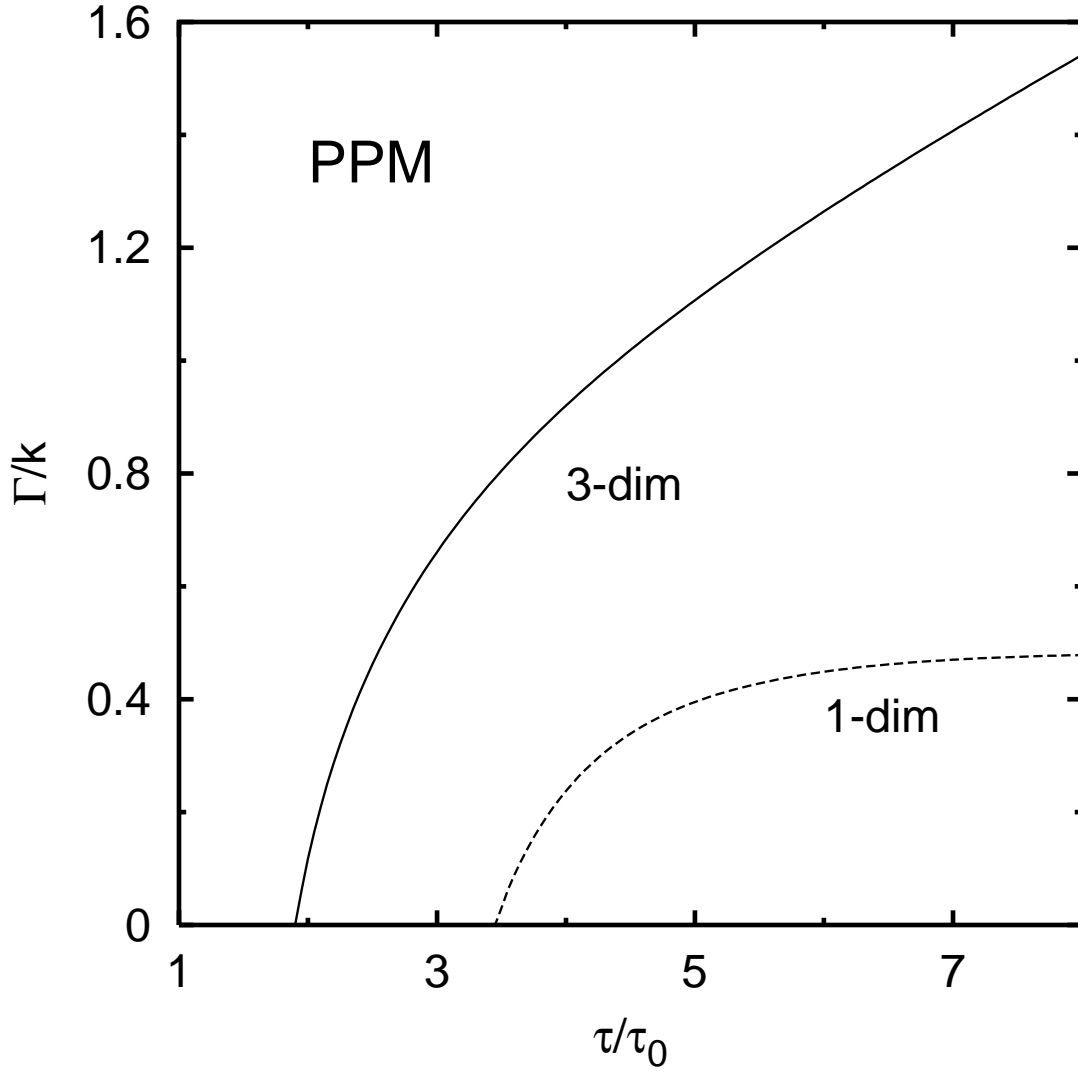


FIG. 12. The instability growth rate Γ/k for a perturbation of the three-dimensional homogeneous expansion (solid line) and for a longitudinal perturbation in the Bjorken expansion (dashed line) as a function of the proper time. Initial conditions like in Fig. 11.

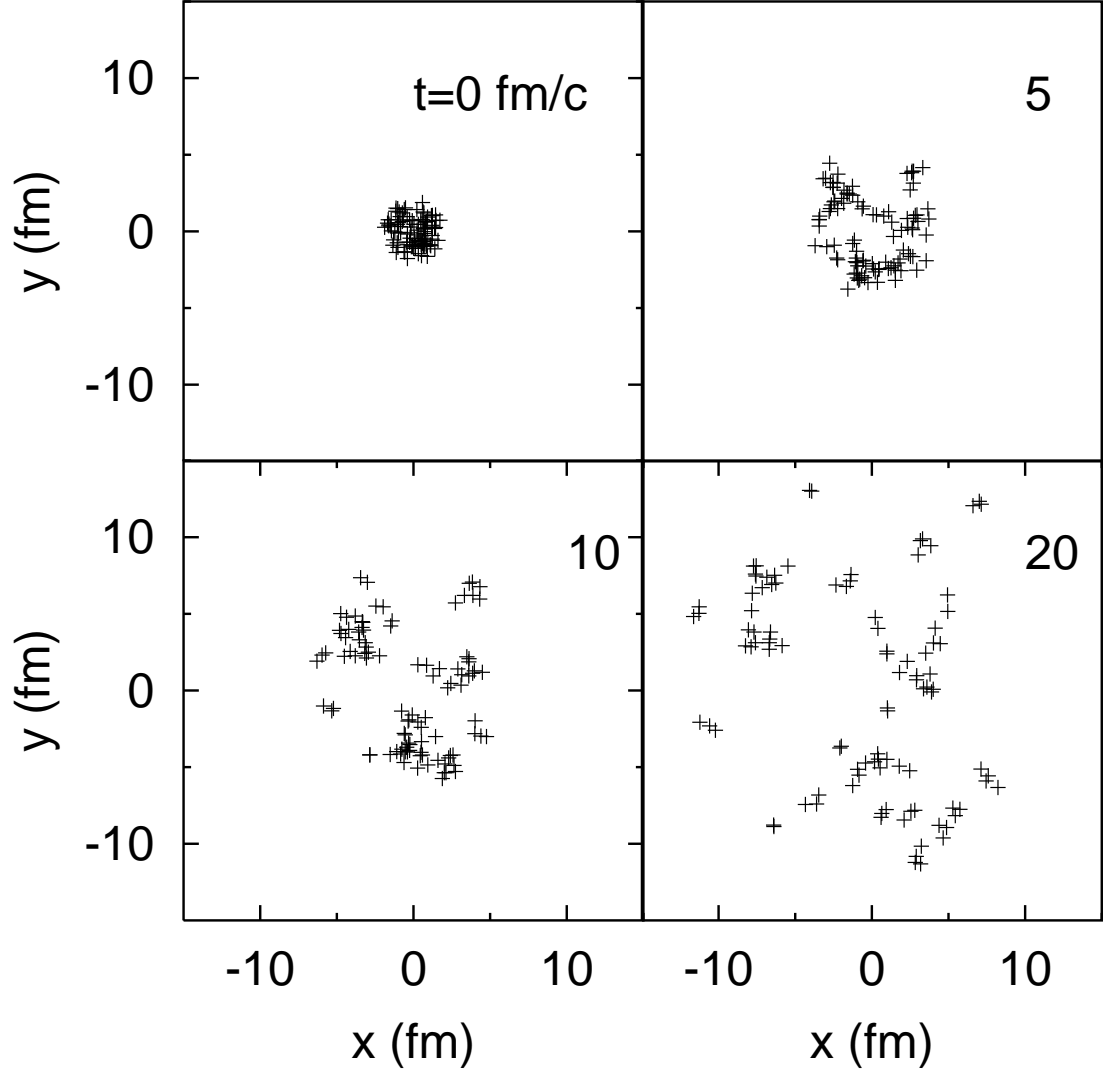


FIG. 13. Expansion of a fireball of partons calculated within molecular dynamics. The positions of the partons with coordinates x and y are projected on the plane $z = 0$. Each cross represents a parton. At $t = 20$ fm/c there is no cluster with a single parton.